Computer Modeling in Engineering & Sciences
DOI:10.32604/cmes.2020.010699
Article

Numerical Characterization of the Annular Flow Behavior and Pressure Loss in Deepwater Drilling Riser

Chengwen Liu[1,*], Lin Zhu[1], Xingru Wu[2,*], Jian Liang[1] and Zhaomin Li[1]

[1]School of Petroleum Engineering, China University of Petroleum (East China), Qingdao, 266580, China
[2]Mewbourne School of Petroleum & Geological Engineering, University of Oklahoma, OK, 73019, USA
*Corresponding Authors: Chengwen Liu. Email: liucw@upc.edu.cn; Xingru Wu. Email: xingru.wu@ou.edu
Received: 21 March 2020; Accepted: 24 April 2020

Abstract: In drilling a deepwater well, the mud density window is narrow, which needs a precise pressure control to drill the well to its designed depth. Therefore, an accurate characterization of annular flow between the drilling riser and drilling string is critical in well control and drilling safety. Many other factors influencing the change of drilling pressure that should be but have not been studied sufficiently. We used numerical method to simulate the process of drill string rotation and vibration in the riser to show that the rotation and transverse vibration of drill string can increase the axial velocity in the annulus, which results in the improvement of the flow field in the annulus, and the effect on pressure loss and its fluctuation amplitude. In addition, there are also multiple secondary flow vortices in the riser annulus under certain eccentricity conditions, which is different from the phenomenon in an ordinary wellbore. The findings of this research are critical in safely controlling well drilling operation in the deepwater environment.

Keywords: Deepwater drilling riser; drill string movement; pressure loss; power-law fluid; numerical simulation

1 Introduction

Advances in drilling and offshore engineering technology enable the exploration and development of hydrocarbon resources from formations with increasing water depth. Compared with drilling in the onshore environment or shallow water, deepwater drilling faces many challenges including the uncertainty of overpressured foramtion, geohazards such as shallow water flow and others [1]. To drill through a formation, the drilling fluid system (mud) density and circulating pressure should be controlled so that the pressure gradient should be greater than the formation pore pressure gradient but be less than the fracturing pressure gradient of the formation. Therefore, frequently managed pressure drilling (MPD) technologies have to be used in the deepwater drilling process [2]. Most of the deepwater reservoirs are over-pressured, which leads to significant challenges in drilling deepwater wells [3,4]. For efficient drilling and minimizing drilling surprises, it is important to accurately characterize the pressure change in the annulus between drilling string and riser or wellbore. Offshore drilling riser insulates seawater and connects the offshore drilling rig and blowout preventer (BOP). Since the mud velocity is inversely proportional to the cross-sectional annulus area and highly impact drilling fluid lifting capacity, the

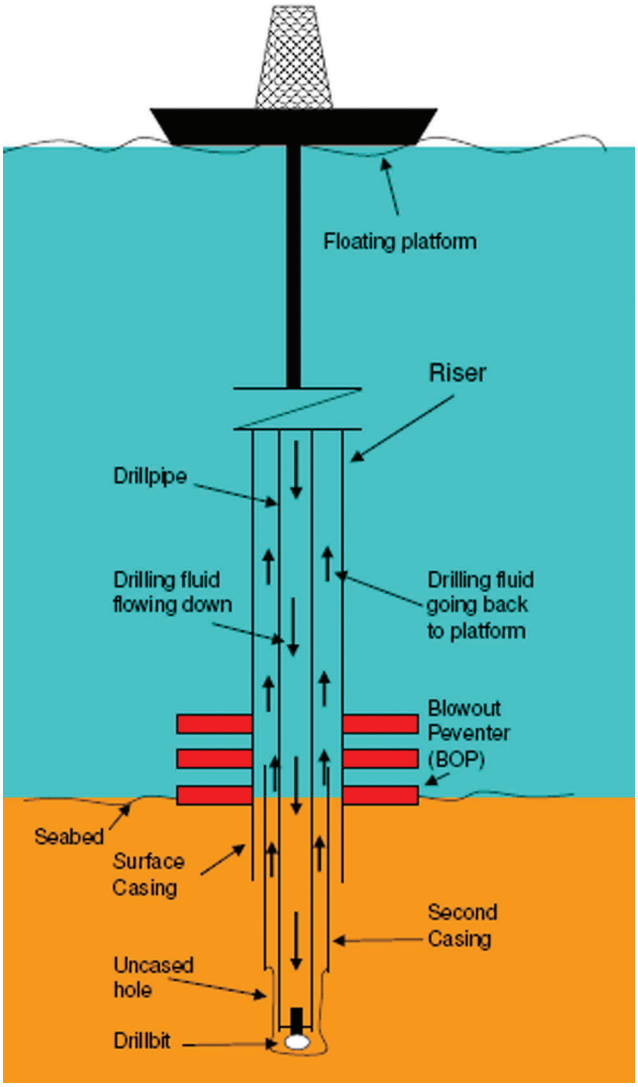

Figure 1: The diagram of deepwater drilling [5]

characterizations of the flow field and pressure change in the annulus should be studied. A diagram of deepwater drilling is shown in the following Fig. 1.

The motion states of the drill string in riser are very complex in the drilling process, including rotation, lateral vibration, axial vibration, torsional vibration, and whirling motion. The complexity is further compounded by the coupling of various forms of vibration and the complex dynamic coupling phenomena between the drill string vibration and riser vibration [6]. Even drilling operation itself can induce riser vibrations [7]. For the offshore drilling, the study on the motion state of a drill string in the riser is very limited and scattered [8–10].

Al-Batati et al. [11] showed that the vortex shedding force would cause the drill string to produce greater lateral displacement and make a periodic motion when the riser is subjected to vortex-induced vibration. In this paper, the flow field characteristics and the annular pressure loss in the coupling movement between the riser and the drill string were studied to describe the velocity field of the annulus more accurately and provide the reference for the well control and analysis of the cuttings carrying problem.

Based on the results of Al-Batati et al. [11] , the coupling motion between the riser and the drill string is simplified as the riser is fixed, and the drill string does periodic transverse vibration in the riser with a fixed amplitude and fixed frequency. The flow dynamic analysis in deepwater drilling is often studied with the finite element method since it is convenient to model complex boundary conditions [12,13]. In this study, we used FLUENT, a commercial computational fluid dynamics software, to simulate the annulus flow field of riser when the drill string is rotating, eccentric and transversely vibrating respectively, the effects of concentric rotation, eccentric rotation and lateral vibration of drill string on the flow field and pressure loss in the riser annulus are obtained.

2 Modeling Annulus Flow of Drilling Fluid

Drilling fluids usually contain bentonite and other additives, which make the drilling fluids exhibit non-Newtonian rheological behavior. Multiple models have been proposed to characterize the mud rheology such as the two-parameter Bingham plastic model or power-law model and three-parameter model such as Herschel-Bulkley model [14]. Water-based polymer muds, especially those made with XC polymer, are best characterized by the two-parameter power-law model because of its simplicity and high accuracy [15]. The constitutive equation of the power-law model is given by Eq. (1):

$$\tau_{ij} = 2K\left(\sqrt{2S_2}\right)^{n-1} S_{ij} \tag{1}$$

where, τ_{ij} is the viscous stress, Pa; K is the consistency coefficient, Pa $\cdot$ s^n; n is the flow behavior index, dimensionless; S_{ij} is the strain rate tensor, s^{-1}; $S_2 = S_{ij}S_{ij}$ is the second invariant of the strain rate tensor.

The drilling fluid is assumed to be isothermal and incompressible, and the flow regime is laminar. Therefore, the continuity equation in a Cartesian coordinate is given by:

$$\frac{\partial u_i}{\partial x_i} = 0 \tag{2}$$

where, u_i is the fluid velocity, m/s; x_i is the position coordinates, m.

The momentum equation is given by:

$$\rho\frac{\partial u_i}{\partial t} + \rho u_j\frac{\partial u_i}{\partial x_j} = \rho f_i - \frac{\partial p}{\partial x_i} + \frac{\partial \tau_{ij}}{\partial x_j} \tag{3}$$

where, ρ is the drilling fluid density, kg/m^3; p is the pressure, Pa; τ_{ij} is the viscous stress, Pa; f_i is the gravity of unit mass, m/s^2.

The bottom inlet condition is set as the velocity inlet of 0.3 m/s (equivalent to a fluid displacement of 57 L/s).The upper outlet is set as the free flow condition, and the wall is assumed no-slip boundary condition. The drilling fluid density is assumed 1200 kg/m^3, the flow consistency index K is 0.43 Pa $\cdot$ s^n, the flow behavior index n is 0.66. The Reynolds number in the annulus is given by:

$$\mathrm{Re}_a = \frac{12^{1-n}\rho\left(D_h - D_p\right)^n {v_a}^{2-n}}{K\left(\dfrac{2n+1}{3n}\right)^n} \tag{4}$$

where, v_a is the average flow velocity in the annulus, m/s; D_h is the riser inner diameter, m; D_p is the outer diameter of the drill string, m; ρ is the drilling fluid density, kg/m^3; K is the consistency coefficient, Pa $\cdot$ s^n; n is the flow behavior index, dimensionless. The Reynolds number in the annulus is 616.5, which belongs to the laminar flow regime.

3 Numerical Simulation of Annulus Flow during Drilling

The geometric model and the meshing of the model when the drill string is concentric are shown in Fig. 2. 135000 hexahedral mesh grid blocks are used in modeling the system, Tab. 1 shows the main input parameters for this study.

The SIMPLEC algorithm is applied to solve the coupled equations of pressure and velocity with FVM. The second-order upwind scheme is used in the convection interpolation algorithm, and the second-order scheme is applied to interpolate pressure. The flow field in the annulus is calculated by the steady method when the drill string with concentric and eccentric rotation respectively. The flow field in the transverse vibration of the drill string is calculated by the unsteady method, and the time step is 0.005 s. Transverse vibration of the drill pipe is realized by dynamic mesh technology.

Table 1: Key parameters of the numerical model for flow velocity field characterization

Inner diameter of riser D_h, m	0.508
Outer diameter of drill string D_p, m	0.127
Riser length L, m	15
Mud density ρ, kg/m^3	1200
Consistency coefficient K, Pa · s^n	0.43
Flow behavior index n	0.66
Mud flow rate Q, L/s	57
Inlet velocity v_a, m/s	0.3
Reynolds number Re$_a$	616.5

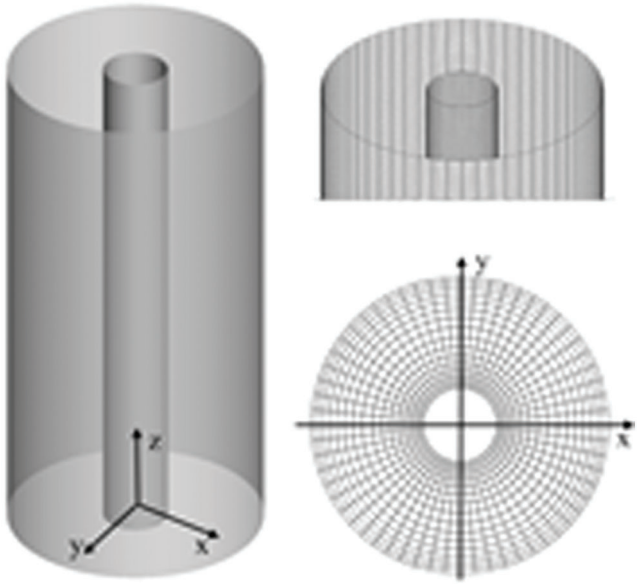

Figure 2: The geometry model and grid meshing

3.1 Effect of Eccentric Drill String Rotation on Flow Field in Annulus

The relative location of the drilling string in the riser affects the velocity and pressure field in the annulus flow, and eccentricity is often used to describe this configuration as shown in Fig. 3. The eccentricity is defined as follows:

$$e = \frac{2\delta}{D_h - D_p} \tag{5}$$

where, δ is the distance between the center of the drill pipe and the center of drilling riser, D_h is the riser inner diameter, D_p is the outer diameter of the drill string. If $e = 0$, this will be concentric flow.

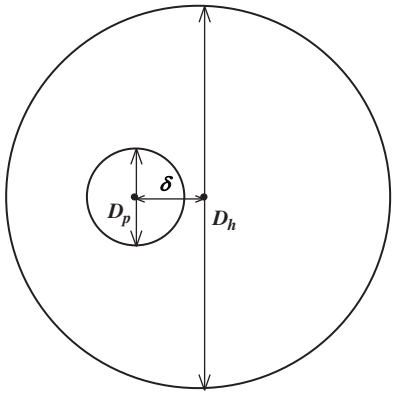

Figure 3: Eccentricity of pipe in pipe structure

Five cases with eccentricities of 0.2, 0.4, 0.6, 0.8 and 1.0 were simulated, respectively. Results are compared with the annular flow field of the concentric drill string (when $e = 0$). Three scenarios are simulated with the drill string rotation speeds of $N = 0$ (stationary), $N = 60$ r/min, and $N = 120$ r/min for all five eccentricities. The contours of axial velocity at the location $z = 7.5$ m are shown in Fig. 4.

Fig. 4 shows that when the drill string does not rotate and is eccentric, the maximum axial velocity of the drilling fluid in the gap of the annulus is larger than that of the concentric, and the velocity in the narrow gap of the annulus is lower. With the increase of eccentricity, the maximum axial velocity of drilling fluid in the wide gap gradually increases, and peaks at the eccentricity $e = 0.6$. Therefore, when the eccentricity is large enough, the axial velocity of drilling fluid can be smaller than the minimum return velocity of cuttings, which will cause some of the cuttings to deposit. When the drill string rotates, the axial flow velocity in the narrow gap will increase, it is a favorable factor to improve the cuttings carrying efficiency of the drilling fluid.

Fig. 5 shows the streamlines of the $z = 7.5$ m section in different drill pipe rotation speeds and different eccentricities. When the drill string rotates, when the eccentricity of the drill string is small, the fluid in the annulus presents a spiral flow, and the spiral direction is the same as the rotation direction of the drill string and the center of spiral flow almost lies in the center of the drill string. With the increase of eccentricity, the flow field in annulus becomes more and more complex. The two spiral secondary flow vortices with the opposite direction of rotation are induced in the annulus, the size of the secondary flow vortex that the rotation direction is the same as the drill string rotation direction increases with the increase of eccentricity, and its position is approximately in the center of the riser. However, with the increase of eccentricity, the center of the secondary flow vortex opposite to the rotation direction of the drill string is gradually shifted to the direction of the drill string, and its size is gradually reduced. When the eccentricity is equal to 1 (i.e., the drill string and riser contact), each side of the drill string will produce a

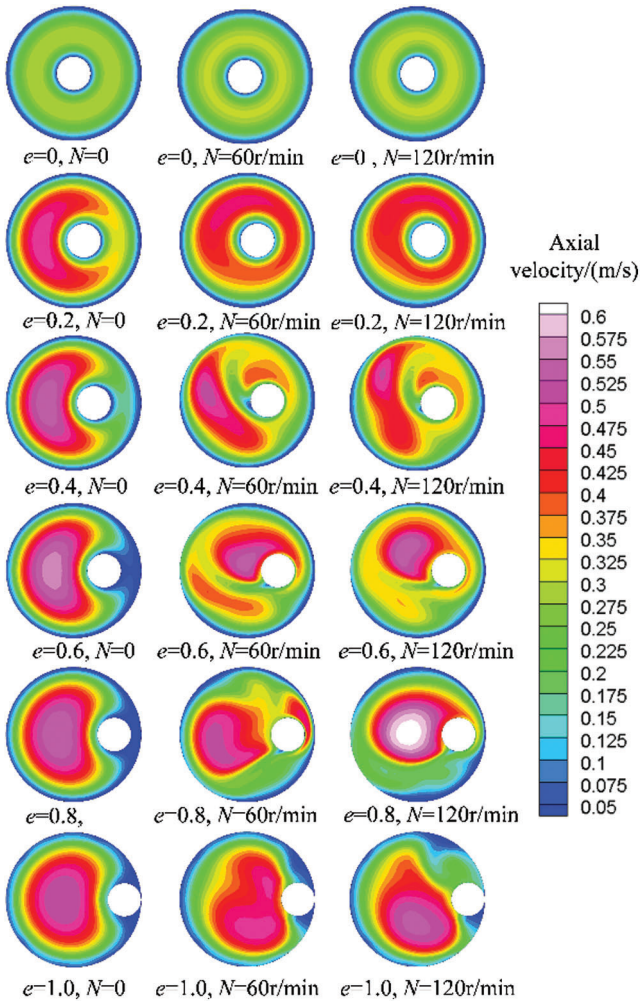

Figure 4: Contours of axial velocity in riser annulus when the drill string is stationary and rotating at different eccentricities (z = 7.5 m)

small vortex in the opposite direction, and most of the area of the annulus is occupied by a secondary flow vortex in the same rotation direction with the drill string. From the above results, we can know because the riser is large, multiple secondary flow vortices rotating in the opposite direction can be induced in the annulus according to the law of conservation of circulation. However, we know only one secondary flow vortex can be induced in the annulus between the drill string and the wellbore from the literature [16]. Therefore, the flow field in the riser is more complex than that in common wellbore annulus.

3.2 Effect of Drill String Vibration on Annular Flow Characteristics

Drill string vibration is a classical problem in drilling engineering and many analytical and numerical types of research have been presented in the literature [17]. When the torsional vibration of the drill string occurs, the velocity field in the annulus of the riser is unsteady. However, the studies on how the vibration affecting the fluid flow dynamics and pressure variation are limited. Assuming the drill string moves left and right periodically along the x-axis and across the center of the riser as Fig. 2. For simplicity, the lateral vibration of the drill string is regarded as a uniform variable motion, so the

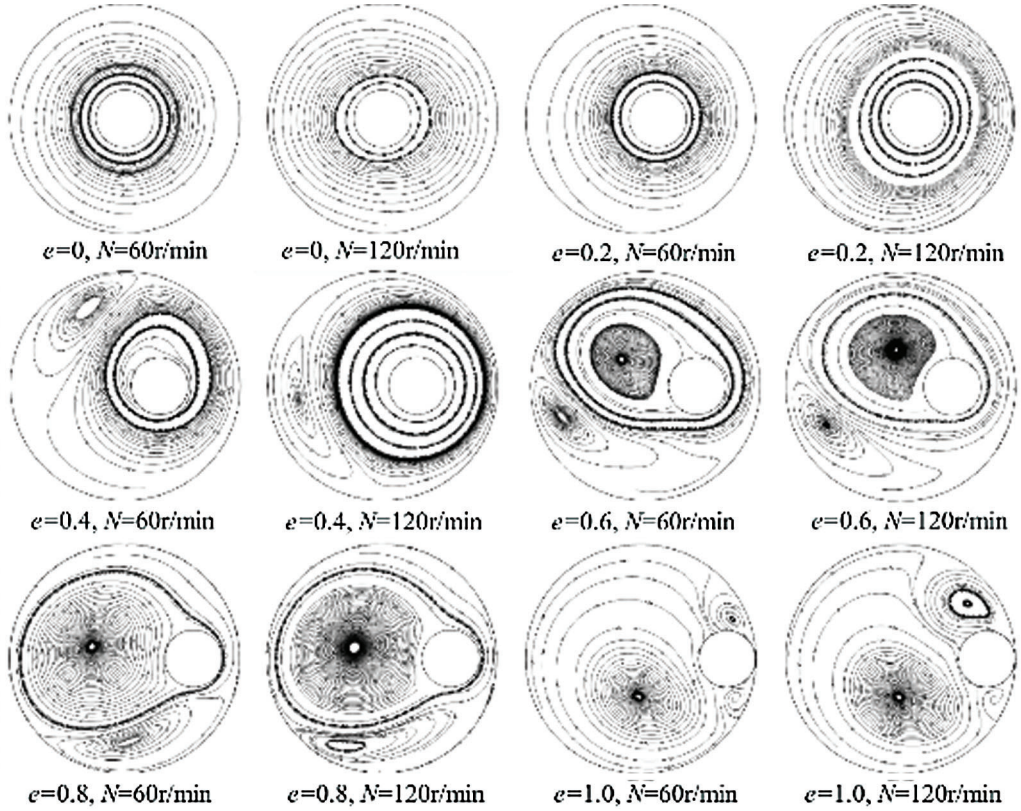

Figure 5: Streamlines in the annulus in different eccentricities and different rotation speeds

displacement-time curve is a quadratic function, the specific equations of motion of the drill string in the x-direction are as follows:

$$s = \begin{cases} -\dfrac{16a}{T^2}\left(t - \dfrac{T}{4}\right)^2 + a\,, & 0 \le t \le \dfrac{T}{2} \\ \dfrac{16a}{T^2}\left(t - \dfrac{3T}{4}\right)^2 - a\,, & \dfrac{T}{2} < t \le T \end{cases} \tag{5}$$

where, s is the displacement of the center of the drill string in the x-direction, m; t is the time, s; a is the amplitude of the drill string in the x-direction, m; T is the lateral vibration period of the drill string in the x-direction, s. According to the above equation, the displacement versus time curve is drawn as shown in Fig. 6.

Fig. 7 shows streamlines in annulus during a vibration period when the amplitude of the drill string is 0.05 m and the period is 2 s. In this condition, the maximum eccentricity of the drill string is 0.262, and the rotation speed of the drill string is 60 r/min (clockwise). It can be seen from Fig. 7 that there exists a spiral secondary flow vortex in the annulus, which is opposite to the direction of rotation of the drill string; meanwhile, with the lateral vibration of the drill string, the secondary flow vortex gradually executes counterclockwise revolution around the center of the riser (the opposite of drill string rotation direction).

Fig. 8 is the distribution of the axial velocity in the annulus within a period of the drill string lateral vibration and compared with Fig. 4. It is found that the instantaneous maximum axial velocity in the annulus is smaller than the maximum axial velocity when the drill string is eccentric but does not rotate, and only slightly larger than the maximum axial velocity when the drill string is concentric but does not

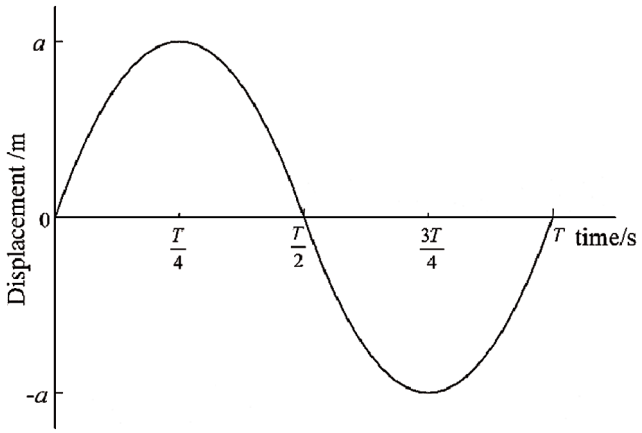

Figure 6: Displacement of the drill string in the *x*-direction over time

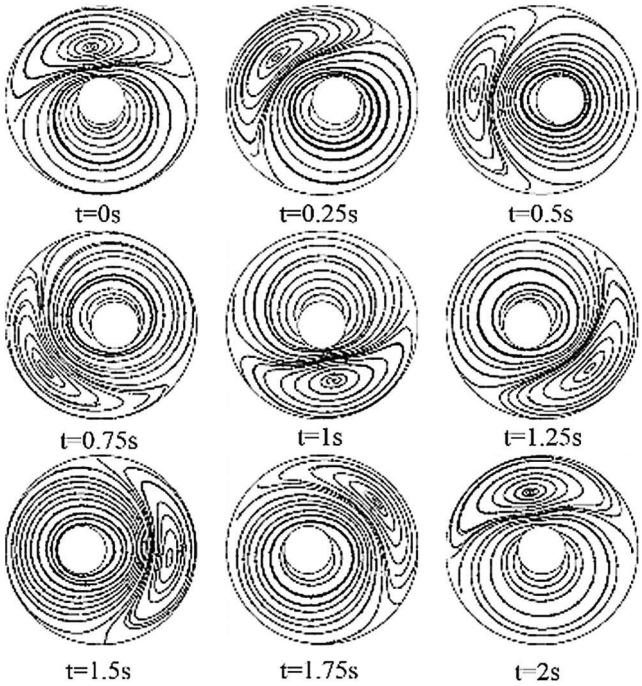

Figure 7: Streamlines in the annulus in a drill string vibration period (z = 7.5 m, a = 0.05 m, T = 2 s)

rotate. Here, the maximum axial velocity during the lateral vibration of the drill string is 0.435 m/s, and the maximum axial velocity is 0.406 m/s when the drill string is concentric but does not rotate. We can also see the velocity difference between the wide gap and narrow gap in the annulus during the lateral vibration of the drill string is much smaller than that of the same eccentricity but no lateral vibration and the axial velocity in the narrow gap is increased, which is a favorable factor for cuttings transport.

3.3 Effect of Drill String Motion on Annular Pressure Loss in Riser

Fig. 9 shows the annular pressure gradient change with the increase of drill string rotation speed for different eccentricities. When the drill string is in stationary, the annular pressure gradient decreases with the increase of eccentricity. When the drill string rotates, the annular pressure gradients for different

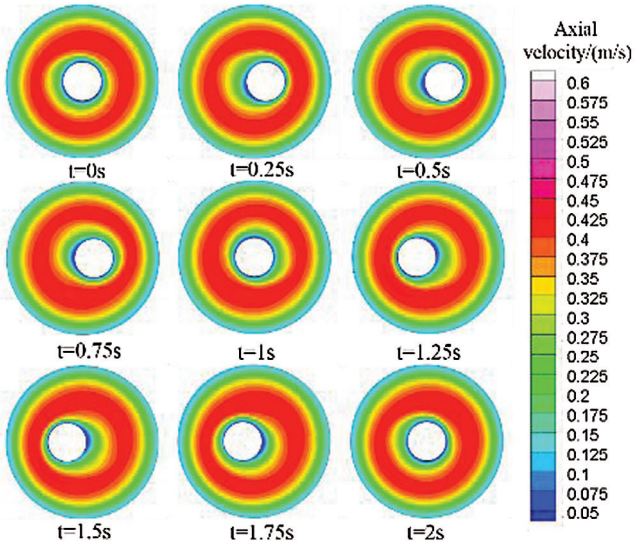

Figure 8: Contours of axial velocity in a drill string vibration period (z = 7.5 m, a = 0.05 m, T = 2 s)

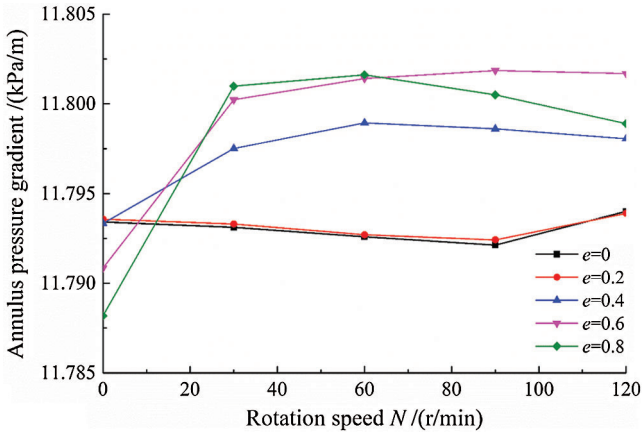

Figure 9: Annular pressure losses in different rotation speeds and different eccentricities

eccentricity increases to a plateau for the scenarios of eccentricity greater than 0.2. In other words, pressure losses in different eccentricities are bigger than that of the concentric annular pressure loss. This may be caused by the secondary flow vortices. Only when the drill string contacts with riser wall (e = 1.0), the annular pressure losses are smaller than that of the concentric annular pressure loss. Overall, in the range of eccentricity and speeds of this study, the effect of the drill string rotation on the annular pressure loss is relatively little, therefore, this effect can be ignored in the calculation of the annular pressure loss of the riser.

In the drilling process, we also studied the lateral vibration frequency and amplitude on the pressure losses for given drill string rotation speed. Here, we assume the rotation speed of 60 r/min clockwise, the annular pressure gradients under the corresponding conditions are shown in Figs. 10 and 11 and Tabs. 2 and 3. As shown Fig. 10 and Tab. 2, when the amplitude of the drill string vibration is constant, the longer the lateral vibration period of the drill string is, the smaller the fluctuation of the pressure loss in the annulus of the riser. The average value of the annular pressure loss is almost constant. From Fig. 11 and Tab. 3, when the drill string vibration period is constant, the greater the amplitude of the drill string vibration is, the higher magnitude of the fluctuation of the annular pressure loss is, and the greater the

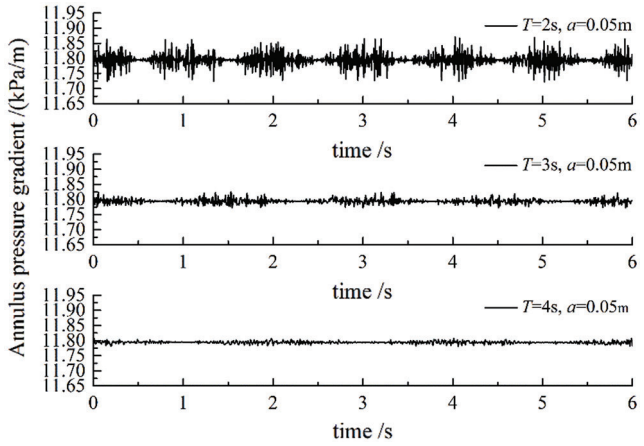

Figure 10: Annular pressure losses in different periods of vibration over time

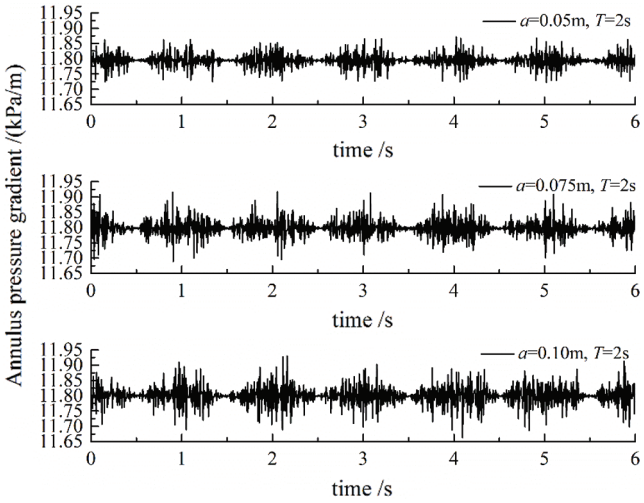

Figure 11: Annular pressure losses in different amplitudes of vibration over time

Table 2: Average value and maximum fluctuating amplitude of the annular pressure losses in different period of vibration (a = 0.05 m)

Drill string lateral vibration period T/s	2	3	4
Maximum amplitude of pressure loss (kPa/m)	0.150	0.052	0.027
Average pressure loss (kPa/m)	11.794	11.794	11.794

average value of the annular pressure loss is. Now a simple estimate of the pressure loss fluctuation is made at a = 0.1 m and T = 2 s: suppose the length of the riser is 1000 m, the maximum magnitude of annular pressure loss fluctuation caused by lateral vibration of the drill string would reach 0.268 MPa, which is converted to an equivalent density of 27.35 kg/m^3. Therefore, to ensure drilling safety with precise control of drilling pressure, the annular pressure loss fluctuation caused by lateral vibration of the drill string should be taken into consideration.

Table 3: Average value and maximum fluctuating amplitude of the annular pressure losses in the different amplitude of vibration ($T = 2$ s)

Drill string vibration amplitude a/m	0.05	0.075	0.1
Maximum amplitude of pressure loss (kPa/m)	0.150	0.228	0.268
Average pressure loss (kPa/m)	11.794	11.798	11.800

4 Conclusions

1. The coupling effect of the rotation and lateral vibration of the drill string can dramatically affect the axial velocity profile in the annulus of the riser. The rotation and lateral vibration of the drill string increases the axial velocity in the narrow gap, reduce the velocity difference between the wide gap and the narrow gap, improve the flow in the narrow gap, and improve the cutting transport effect.
2. The rotation and lateral vibration of the drill string complicate the flow pattern in the riser annulus by inducing secondary vortices in the riser annulus. When the drill string rotates eccentrically, the number of secondary vortices increases with the increase of eccentricity.
3. When the drill string is rotating, the pressure loss of eccentric annulus is greater than that of the concentric annulus, but the effect of drill string rotation on the pressure loss of annulus is relatively small, so this effect can be ignored in practice. The annular pressure loss fluctuates with the transverse vibration of the drill string. The influence of the vibration amplitude on the average value and amplitude of the pressure loss is greater than that of the vibration period. With the increase of the vibration amplitude of the drill string, the fluctuation amplitude and average value of the annular pressure loss increase. Therefore, the influence of transverse vibration of drill string on the annulus pressure loss should be considered in the well control design of deep-water drilling.

Funding Statement: The research work in this paper is supported by the National Natural Science Foundation of China (Grant No. U1762211), National Key Technologies R & D Program of China (Grant No. 2016ZX05022-005), This research is also partially supported by Tubular Goods Research Institute of CNPC and State Key Laboratory of Performance and Structural Safety for Petroleum Tubular Goods and Equipment Material of China National Petroleum Corporation.

Conflicts of Interest: The authors declare that they have no conflicts of interest to report regarding the present study.

References

1. Shaughnessy, J. M., Daugherty, W. T., Graff, R. L., Durkee, T. (2007). More ultra-deepwater drilling problems, *The 2007 SPE/IADC Drilling Conference, February 20–22*, Amsterdam, The Netherlands.
2. Nas, S. W. (2010). Deepwater managed pressure drilling applications. *The CPS/SPE International Oil & Gas Conference and Exhibition*, *June 8–10*, Beijing, China.
3. Marland, C. N., Nicholas, S. M., Cox, W., Flannery, C., Thistle, B. (2013). Pressure prediction and drilling challenges in a deepwater subsalt well from offshore Nova Scotia, Canada. *SPE Drilling & Completion, 22(03),* 227–236. DOI 10.2118/98279-PA.
4. Willson, S., Edwards, S., Heppard, P. D., Li, X., Coltrin, G. et al. (2003). Wellbore stability challenges in the deep water, Gulf of Mexico: case history examples from the pompano field. *The SPE Annual Technical Conference and Exhibition October 5–8*, Denver, Colorado, USA.
5. EnggCyclopedia. (2011). Riser. *https://www.enggcyclopedia.com/2011/11/riser/*.
6. Wang, S., Xu, X., Lu, X. (2016). Movement optimization of freely-hanging deepwater risers in reentry. *Ocean Engineering, 116,* 32–41. DOI 10.1016/j.oceaneng.2016.02.029.

7. Blevins, R. D., Coughran, C. S., Utt, M. E., Raghavan, K. (2016). Drilling-induced riser vibration. *International Journal of Offshore and Polar Engineering, 27(3),* 232–238. DOI 10.17736/ijope.2017.jc702.
8. Fu, Q. C. (2016). Numerical simulation of pressure loss in large size annulus of deepwater drilling riser. *Materials Science Forum, 857,* 590–597. DOI 10.4028/www.scientific.net/MSF.857.590.
9. Sher, F., Ahmed, S., Asghar, U. (2017). Suppression of vortex induced vibrations in marine risers by fairings, *14th International Bhurban Conference on Applied Sciences and Technology, January 10–14*, Islamabad, Pakistan.
10. Claro, C., Cruz, I., Karunakaran, D., Hepener, G., Ji, C. et al. (2016). Hydrodynamic behavior of an ultra-deep water decoupled buoy supporting risers. *35th International Conference on Ocean, Offshore and Arctic Engineering, Busan, South Korea*.
11. Al-Batati, N., Hashim, F. M., Pao, K. S. (2014). Simulation of drill string vibration inside well bore due to riser's oscillation. *Research Journal of Applied Sciences, Engineering and Technology, 7(1),* 174–182. DOI 10.19026/rjaset.7.237.
12. Downton, G. (2015). Systems modeling and design of automated-directional-drilling systems. *SPE Drilling & Completion, 30(3),* 212–232. DOI 10.2118/170644-PA.
13. Guo, Y. G., Blanford, M., Candella, J. (2015). Evaluating the risk of casing failure caused by high-density perforation: a 3D finite-element-method study of compaction-induced casing deformation in a deepwater reservoir, Gulf of Mexico. *SPE Drilling & Completion, 30(2),* 141–151. DOI 10.2118/170618-PA.
14. Kelessidis, V., Maglione, R., Tsamantaki, C., Aspirtakis, Y. (2006). Optimal determination of rheological parameters for Herschel-Bulkley drilling fluids and impact on pressure drop, velocity profiles and penetration rates during drilling. *Journal of Petroleum Science and Engineering, 53(3–4),* 203–224. DOI 10.1016/j.petrol.2006.06.004.
15. Graham, D., Jones, T. (1994). Settling and transport of spherical particles in power-law fluids at finite Reynolds number. *Journal of Non-Newtonian Fluid Mechanics, 54(6),* 465–488. DOI 10.1016/0377-0257(94)80037-5.
16. Escudier, M. P., Oliveira, P. J., Pinho, F. T. (2002). Fully developed laminar flow of purely viscous non-Newtonian liquids through annuli, including the effects of eccentricity and inner-cylinder rotation. *International Journal of Heat and Fluid Flow, 23(1),* 52–73. DOI 10.1016/S0142-727X(01)00135-7.
17. Karkoub, M., Abdel-Magid, Y. L., Balachandran, B. (2009). Drill-string torsional vibration suppression using GA optimized controllers. *Journal of Canadian Petroleum Technology, 48(12),* 32–38. DOI 10.2118/132161-PA.